ARTICLE OPEN

Cohesin haploinsufficiency and inv(16) cooperate to reinforce Fli1 gene transcriptional programs during acute myeloid leukemia initiation and maintenance

Alison E. Meyer[1,11], Katelyn E. Heimbruch[2,11], Kirthi Pulakanti[1], Cary Stelloh[1], Nataly Cruz-Rodriguez[1], Josiah Murray[3], Dandan Wang[1], Lisa Latzko[4,5,6], Sebastian Vosberg[4], Philipp A. Greif[4,5,6], Lucio H. Castilla[7], John A. Pulikkan[1,3], Subramaniam Malarkannan[1,8,9] and Sridhar Rao[1,3,10]✉

© The Author(s) 2026

Core binding factor (CBF) acute myeloid leukemias typically harbor the translocations t(8;21) or inv(16). As cohesin mutations are less commonly observed with inv(16) than with t(8;21), we hypothesized that they may negatively impact inv(16)-driven AML. Using a mouse model of inv(16) with haploinsufficiency of the cohesin subunit *Smc3*, we paradoxically found that inv(16); *Smc3*$^{\Delta/+}$ mice have a reduced leukemic latency compared to inv(16); *Smc3*$^{+/+}$ mice, disproving our initial hypothesis and instead suggesting a role for cohesin loss in enhancing inv(16)-driven disease. Consistent with the known role of cohesin haploinsufficiency in altering chromatin accessibility, we demonstrated an increase in chromatin accessibility in inv(16); *Smc3*$^{\Delta/+}$ hematopoietic stem and progenitor cells (HSPCs) prior to leukemia development, with an enrichment for Fli1 DNA binding motifs. Through scRNA-seq on pre-leukemic HSPCs, we observe an increase in *Fli1* expression and enhanced Fli1 target expression in ST-HSCs. We further show that Fli1 is essential for the maintenance stage of inv(16); *Smc3*$^{\Delta/+}$ AML. Our data demonstrate a role for cohesin loss in enhancing the aggressiveness of inv(16)-driven AML and identify Fli1 as a previously unrecognized therapeutic vulnerability in cohesin-mutated AML.

Leukemia; https://doi.org/10.1038/s41375-026-03070-6

INTRODUCTION

Acute myeloid leukemia (AML) is a bone marrow cancer affecting ~20,000 people annually in the United States, with global rates of incidence and mortality rising [1]. Multiple studies utilizing whole genome or whole exome sequencing on patient samples have identified causal or contributing mutations [2–6] and have revealed a genetically diverse disease [4]. On average, each patient carries 5–15 different mutations [4] and therefore has a unique landscape of somatic mutations and clonal composition. How acquired mutations work together to initiate the transformation to leukemia and/or maintain the disease is a critical knowledge gap in AML. Thus, further study has the potential to identify novel therapeutic pathways.

Approximately 15% of adult AML patients have mutations in the core binding factor complex [7–10]. Core binding factor (CBF) is a heterodimeric transcriptional complex comprised of RUNX1, 2, or 3 and CBFβ. This complex is critical for establishing and maintaining hematopoietic stem cells and regulating differentiation through the recruitment of lineage-specific transcription factors [7–10]. Both subunits can be altered through translocations in AML, with RUNX1 being the target in *t*(8;21) and CBFβ in inv(16) [9, 11]. These chromosomal aberrations result in the expression of the fusion proteins RUNX1::RUNX1T1 (also known as AML1::ETO) in *t*(8;21) and CBFβ::SMMHC in inv(16). Either mutation is necessary but not sufficient for leukemogenesis, and multiple secondary or tertiary mutations can influence the rate of disease initiation or progression [7, 8, 11, 12]. Interestingly, while both fusion proteins are classically thought to act in a dominant negative manner toward native RUNX1 [10, 11, 13, 14], the co-mutational and transcriptional profiles of *t*(8;21) and inv(16) AMLs differ [14–19], and they often have different French-American-British classifications [8]. Thus, while the two core binding factor AMLs are usually classified together clinically and are typically considered favorable, they are often morphologically and genetically distinct.

Of note, mutations in the cohesin complex are predominantly found in *t*(8;21) AMLs at a rate of 18–27% [15–19]. By contrast, cohesin complex mutations have not been readily detected in inv(16) AMLs [15–19]. The cohesin complex is a four-member ring-like complex comprised of the subunits SMC1A, SMC3, RAD21, and STAG2. Cohesin's canonical function is to maintain sister

[1]Versiti Blood Research Institute, Milwaukee, WI, USA. [2]Pediatric Residency Program, Cincinnati Children's Hospital, Cincinnati, OH, USA. [3]Department of Cell Biology, Neurobiology, and Anatomy, Medical College of Wisconsin, Milwaukee, WI, USA. [4]Department of Medicine III, University Hospital, LMU Munich, Munich, Germany. [5]German Cancer Consortium (DKTK), Munich, Germany. [6]German Cancer Research Center (DKFZ), Heidelberg, Germany. [7]Department of Molecular, Cell and Cancer Biology, University of Massachusetts Chan Medical School, Worcester, MA, USA. [8]Department of Medicine (Hematology and Oncology), Medical College of Wisconsin, Milwaukee, WI, USA. [9]Department of Microbiology & Immunology, Medical College of Wisconsin, Milwaukee, WI, USA. [10]Department of Pediatrics, Division of Hematology, Oncology, and Bone Marrow Transplantation, Medical College of Wisconsin, Milwaukee, WI, USA. [11]These authors contributed equally: Alison E. Meyer, Katelyn E. Heimbruch. ✉email: sridhar.rao@versiti.org

Received: 3 February 2025 Revised: 23 June 2026 Accepted: 10 July 2026
Published online: 27 July 2026

chromatid cohesion; it also has well-documented roles in regulating chromatin looping and gene transcription [20, 21]. Cohesin mutations occur in AML at a rate of 10%, are mutually exclusive, and typically result in haploinsufficiency of the complex [3, 22–24]. Because AMLs harboring cohesin mutations show low levels of aneuploidy, disruption of their canonical function is not thought to contribute to disease [25–28]. Instead, cohesin mutations have been hypothesized to disrupt gene regulation in AML [21]. Due to the reported low co-occurrence of cohesin mutations with inv(16) in leukemia, we originally hypothesized that cohesin haploinsufficiency would be detrimental to inv(16) leukemogenesis or progression. In contrast to our hypothesis, we found that *Smc3* haploinsufficiency significantly decreased AML latency in inv(16) mice. Our data suggest that cohesin mutations increase the accessibility of binding sites for the transcription factor Fli1 in pre-leukemic cells. This results in enhanced Fli1 target gene expression, likely contributing to accelerated inv(16)-driven disease. Our data further identify Fli1 as a potential therapeutic vulnerability in inv(16) and cohesin-mutated AMLs.

MATERIALS AND METHODS

A detailed materials and methods section can be found in the Supplementary Material

RESULTS

Smc3 haploinsufficiency decreases the latency of inv(16) AML

We initially hypothesized that cohesin haploinsufficiency would delay or prevent inv(16)-driven AML, as cohesin mutations and inv(16) are rarely co-occurrent. To test this hypothesis, we combined the inducible inv(16)$^{+/56M}$ [29] and *Smc3*$^{fl/+}$ mouse models [26]. In these models, heterozygous expression of inv(16) and loss of one allele of *Smc3* are driven by Mx1-Cre activation following pIpC injection, resulting in an approximate 50% loss of Smc3 expression [26, 30](Supplementary Fig. 1A). We monitored 15 inv(16)$^{+/56M}$; *Smc3*$^{+/+}$ (referred to as inv(16); *Swt*) and 24 inv(16)$^{+/56M}$; *Smc3*$^{\Delta/+}$ mice (referred to as inv(16); *Shet*) for AML development following pIpC injection (Fig. 1A). Moribund mice were euthanized, and AML was confirmed when possible by staining of bone marrow samples, the presence of pale bones, hepatosplenomegaly, and the disruption of normal liver and spleen structure (Fig. 1B and Supplementary Fig. 1B–D). While AML was 100% penetrant in both genotypes, in contrast to our hypothesis, we observed a statistically significant decrease in latency in inv(16); *Shet* mice (14 weeks) compared to inv(16); *Swt* mice (20 weeks, Fig. 1A), suggesting *Smc3* haploinsufficiency facilitates accelerated inv(16)-driven disease. Leukemias from both genotypes were morphologically similar (Fig. 1B), the mice displayed similar hepatosplenomegaly and blast infiltration of the liver/spleen (Supplementary Fig. 1B–D), and the leukemias were similarly differentiated as measured by flow cytometry (Supplementary Fig. 1E). Our data collectively disprove our initial hypothesis and instead suggest that *Smc3* haploinsufficiency and inv(16) cooperatively decrease disease latency through effects on either the rate of leukemic transformation or disease progression.

Smc3 haploinsufficiency increases chromatin accessibility at ETS family binding sites in pre-leukemic inv(16) HSPCs

To examine how cohesin mutations might contribute to inv(16)-mediated leukemic transformation, we performed several studies on pre-leukemic hematopoietic stem and progenitor cells (HSPCs, Lin-). Because cohesin has a known role in chromatin accessibility, we first performed ATAC (Assay for Transposase-Accessible Chromatin) sequencing. HSPCs were isolated from Cre- mice and were infected with retrovirus expressing tamoxifen-inducible Cre. Cre expression was induced 48 h after infection by administration of 4-hydroxytamoxifen. Knock-in of inv(16) and excision of one *Smc3* allele were confirmed by genotyping, and ATAC sequencing was performed. We found an increased number of accessible chromatin sites in inv(16); *Shet* vs. inv(16); *Swt* HSPCs (Fig. 2A). Specifically, 33 133 accessible regions were unique to inv(16); *Shet* compared to 564 regions unique to inv(16); *Swt* (Fig. 2A and Supplementary Table 1), demonstrating that cohesin haploinsufficiency promoted a dramatic increase in the number of accessible sites detected. As cohesin mutations have been linked to alterations in hematopoietic transcription factor site accessibility [26–28, 31], we next performed a de novo motif analysis using HOMER to determine which transcription factor binding sites were enriched in the unique peaks in inv(16); *Shet* cells. Along with CTCF, which is well known to co-regulate chromatin organization with cohesin, the top 10 most enriched transcription factor sites included the AP-1 superfamily members Fos, Fra1, and Fra2, and multiple ETS family transcription factor members (Etv1, Etv4, Fli1, Elf5, PU.1, and Elf4; Fig. 2B). Because cells may have differentiated during retroviral infection with Cre, we verified our ATAC-seq results with freshly-isolated HSPCs following pIpC treatment. HOMER analysis again revealed the enrichment of ETS family transcription factors in inv(16);*Shet* differentially accessible chromatin regions (Supplementary Fig. 2), confirming that *Smc3* haploinsufficiency results in increased chromatin accessibility at ETS binding sites.

The fusion protein resulting from inv(16), CBFβ::SMMHC, has been shown to interact with WT RUNX1 and the critical myeloid ETS transcription factors FLI1, ERG, PU.1, and ELF1 at promoter regions to regulate gene expression [10, 32], making the enrichment of ETS family motifs intriguing. Furthermore, we observed similar ATAC-seq results in a second model of co-mutational AML that we have previously studied, where the *Npm1*$^{cA/+}$ mutation was combined with *Smc3*$^{\Delta/+}$ (Fig. 2C) [30]. HOMER analysis revealed the top five enriched motifs in the *Npm1*$^{cA+}$; *Shet* uniquely accessible chromatin regions were all ETS family transcription factors (Fig. 2D). Given that ETS factor site accessibility was consistent with *Smc3* haploinsufficiency across two separate driver oncogene models and in several published cohesin models [26, 28], we further examined the impact of ETS family transcription factors on inv(16) HSPC biology.

Smc3 haploinsufficiency increases Fli1 expression and enhances Fli1 activity in pre-leukemic inv(16) HSPCs

As accessible chromatin is generally associated with active transcription, we reasoned that elevated expression levels of ETS family transcription factors may contribute to gene dysregulation. Of the ETS factors in our top 10 most enriched sites in inv(16); *Shet* accessible chromatin (Fig. 2B), Etv1, Etv4, Fli1, Elf4, and PU.1 (encoded by *Spi1*) are known to be expressed in hematopoietic cells, while Elf5 is largely expressed in epithelial cells and was thus not considered further. The ETS domain, which facilitates DNA binding, is 96% identical between Erg and Fli1 [33], making separation of their effects difficult. For this reason, we included Erg in further analyses. Our ATAC-seq data revealed increased chromatin accessibility near the transcription start site (TSS) of *Fli1*, *Elf4*, *Etv4*, and *Spi1*, but not in *Etv1* or *Erg*, in inv(16); *Shet* vs. *Swt* cells (Fig. 2E and Supplementary Fig. 3A, B, C and data not shown), consistent with increased gene expression. For *Fli1*, additional uniquely accessible chromatin regions were present in inv(16); *Shet* cells, with a peak approximately 10 kb upstream of the TSS and several throughout the gene body (Fig. 2E).

Given the increased accessibility of genes encoding Ets family members, we performed qPCR to quantify mRNA levels of these genes in inv(16); *Swt* and *Shet* HSPCs. Interestingly, only *Fli1* and *Erg* mRNA were significantly upregulated in inv(16); *Shet* vs. inv(16); *Swt* HSPCs (Fig. 3A and Supplementary Fig. 4A), however only Fli1 was upregulated at the protein level (Fig. 3B and Supplementary Fig. 4B). We also assayed the expression levels of several known Fli1 target genes and found *Ccl2*, *Ccng1*, *Mdm2*,

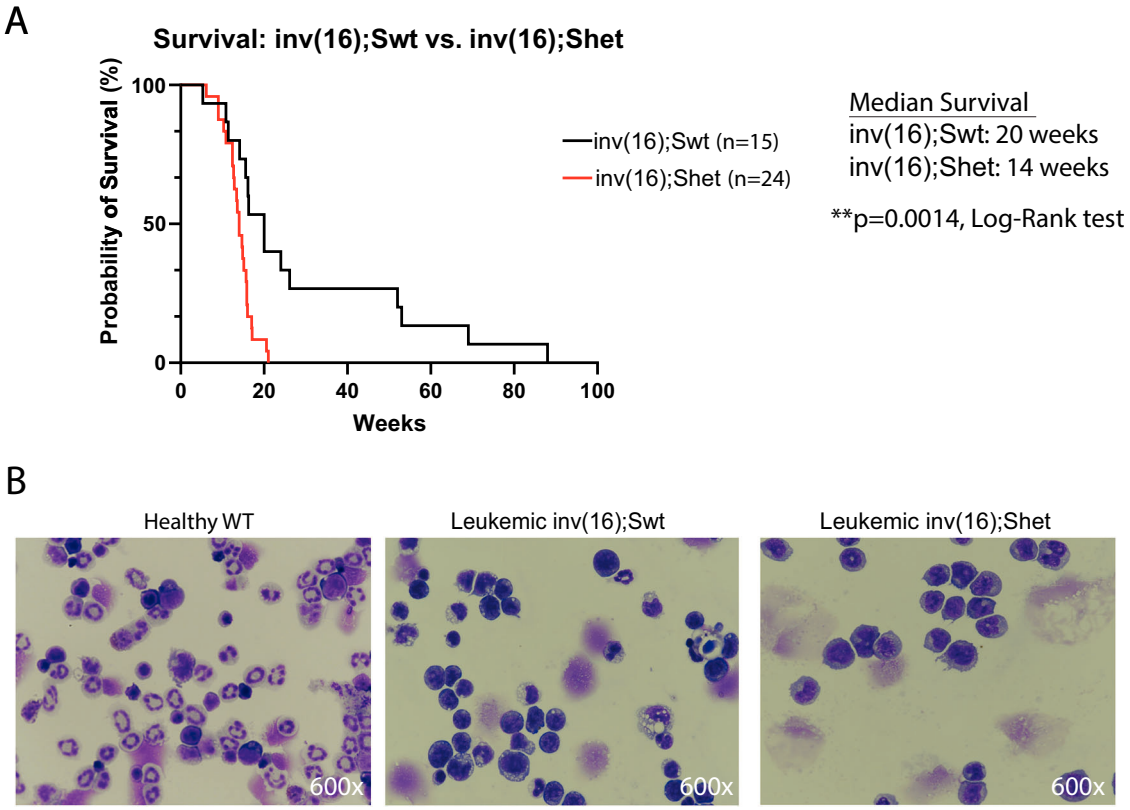

Fig. 1 ***Smc3* haploinsufficiency decreases the latency of inv(16)-driven AML. A** Survival curve showing decreased latency of inv(16); *Shet* mice (red line) vs. inv(16); *Swt* mice (black line). $^{**}p < 0.01$, log-rank test. **B** Examples of bone marrow from a healthy wildtype (WT) animal (left panel), a leukemic inv(16); *Swt* (middle panel), and a leukemic inv(16); *Shet* animal (right panel). Images taken at 600x.

Rab27b, and *Lmo2* were upregulated in inv(16); *Shet* vs. inv(16); *Swt* HSPCs (Fig. 3C). Collectively, this work demonstrates that the Fli1 protein is overexpressed and drives the increased expression of known target genes in *Smc3* haploinsufficient inv(16) HSPCs.

Given the enrichment of Fli1 binding sites in uniquely accessible chromatin in inv(16) *Shet* HSPCs, we hypothesized that such sites may identify pathways of potential importance to AML transformation. To this end, we identified chromatin accessible regions present only in inv(16);*Shet* and isolated those with a consensus binding motif for Fli1 using the HOMER motif discovery tool. We next mapped these sites to their nearest genes within +/− 50 kb and performed genome ontology (GO) pathway analysis using the ShinyGO gene set enrichment tool (Supplementary Table 2). Interestingly, the top five enriched pathway terms associated with Fli1 binding sites in the unique inv(16); *Shet* accessible chromatin included "Ras signaling pathway" (Fig. 3D). Several Ras pathway genes including *Pla2g6*, *Kit*, *Igf1r*, and *Insr* showed increased accessibility near the TSS in inv(16); *Shet* vs. inv(16); *Swt* cells (Supplementary Fig. 5A, B and data not shown). Of note, the most common co-occurring mutations in inv(16) AMLs are in *NRAS* and *KRAS*, which are less common in *t(8;21)* [15–19]. However, active RAS activity levels were similar in inv(16); *Swt* and inv(16); *Shet* HSPCs (Supplementary Fig. 5C), suggesting that *Smc3* haploinsufficiency does not result in the direct activation of RAS itself. Instead, our data suggest that a subset of genes downstream of RAS activation may be similarly regulated by Fli1 in pre-leukemic inv(16); *Shet* cells.

Other interesting GO pathways included "pathways in cancer", "cytokine-cytokine receptor interaction", and "human cytomegalovirus infection" (Fig. 3D), which were comprised of overlapping gene sets with known links to the regulation of AML (ex, cell cycle, apoptosis, and immune signaling; Supplementary Table 2). Collectively, our data suggest that *Smc3* haploinsufficiency results in increased chromatin accessibility at Fli1 transcription factor binding sites and elevated Fli1 target expression, which increases RAS and other cancer-associated gene expression pathways in inv(16) HSPCs and may contribute to an increased rate of leukemogenesis.

Fli1 is overexpressed and drives an enhanced gene expression program in inv(16); Shet HSCs

As AML is thought to originate with mutations in hematopoietic stem cells or myeloid progenitors [34–37], we hypothesized that *Fli1* and its effector genes would be differentially expressed in the most primitive hematopoietic cells. To address this hypothesis, we sorted Lin-, Sca1 + , c-Kit+ (LSK) cells from two independent inv(16); *Swt* and inv(16); *Shet* animals four weeks post-pIpC treatment and analyzed these cells by scRNA sequencing, prior to the animals developing AML. The LSK population contains short and long-term-hematopoietic stem cells (ST/LT-HSCs) and multipotent progenitors (MPPs) [38–40]. Cells clustered into nine main groups, with all groups containing cells from both genotypes (Fig. 4A and Supplementary Fig. 6A). Cells were annotated using the Haemopedia mouse RNAseq database [41]. Only cells that were annotated as MPPs (Lin-, Sca1 + , c-Kit + , CD34 + , Flt3 +) and ST-HSCs (Lin-, Sca1 + , c-Kit + , CD34 + , Flt3-; hereafter referred to as HSCs) were retained. We were unable to identify LT-HSCs due to their low frequency, consistent with their lack of expansion in inv(16) mice [42]. In total, we analyzed 5 499 inv(16); *Swt* cells and 2 557 inv(16); *Shet* cells, which were separated into the MPP and HSC populations as shown in Table 1 and Fig. 4B. Cells were next analyzed for *Fli1* expression based on cluster (Supplementary Fig. 6B). We found a significant upregulation of *Fli1* in inv(16); *Shet* cells vs. inv(16); *Swt* cells in clusters 0, 1, 3, and 6 (Fig. 4C and Supplementary Table 3). *Fli1* expression in clusters 2, 4, 5, 7 and 8 was not statistically different between genotypes (Supplementary

A

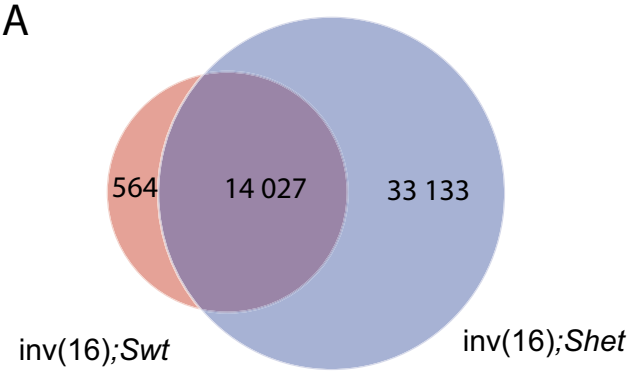

B

TF	Motif	P-value
CTCF		1e-637
ETV1		1e-584
ETV4		1e-457
FLI1		1e-439
ELF5		1e-430
FRA1		1e-417
FOS		1e-415
FRA2		1e-407
PU.1		1e-406
ELF4		1e-405

C

D

TF	Motif	P-value
ETV1		1e-322
FLI1		1e-319
ETS1		1e-306
ERG		1e-304
ETV2		1e-290

E

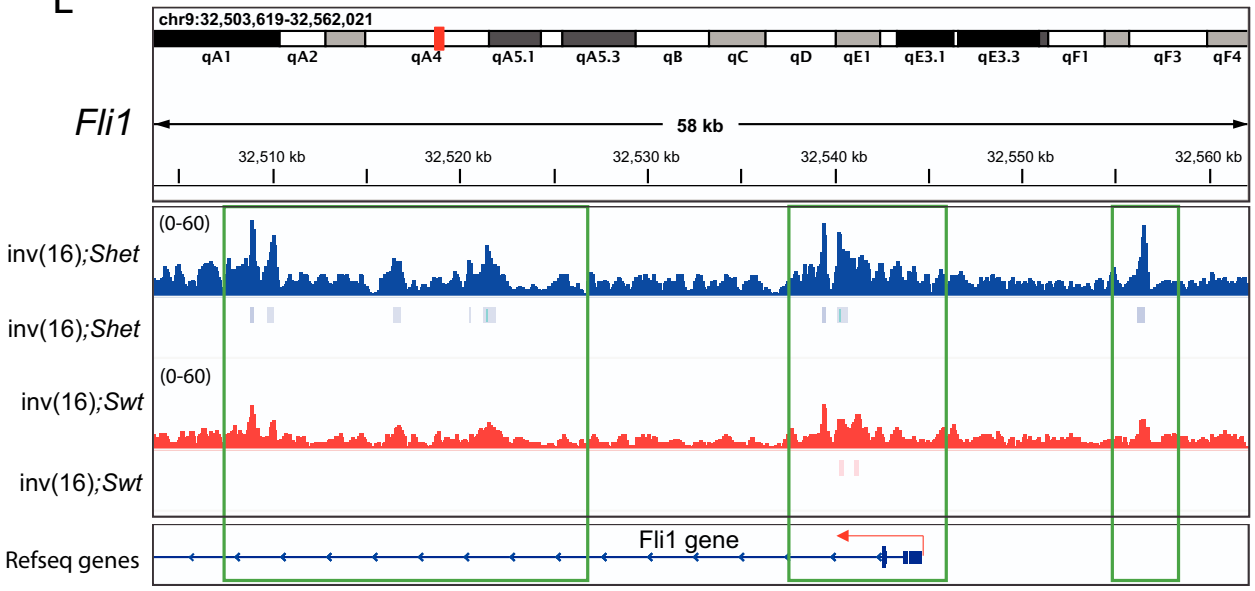

Fig. 6C). Interestingly, when examined by cell type, although a trend toward increased *Fli1* expression was observed in MPPs, this expression increase reached statistical significance only in HSCs (Fig. 4D). Collectively our data indicate that, while the overall cell types and numbers between inv(16)*Shet* and inv(16); *Swt* were similar, inv(16); *Shet* HSCs showed elevated *Fli1* mRNA.

To determine if the increased expression of Fli1 was associated with increased expression of its target genes, or regulon, we applied the single-cell regulatory network inference and clustering (pySCENIC) program [43] to our scRNA sequencing data to identify transcription factor-driven regulons that were different between the two genotypes [43]. The activity of hundreds of regulons was

Fig. 2 *Smc3* haploinsufficiency increases chromatin accessibility at ETS family binding sites in pre-leukemic inv(16) HSPCs. A ATAC replicates were combined for all analyses ($n = 3$ for both genotypes). Venn diagram showing the number of shared and uniquely identified accessible chromatin peaks in inv(16);*Swt* (red) and inv(16);*Shet* (blue) HPSCs by ATAC sequencing. **B** HOMER analysis of the unique peaks in inv(16);*Shet* HPSCs shows ETS family transcription factor sites are prevalent in the top ten most enriched motifs by *p*-value. **C** ATAC replicates were combined for all analyses ($n = 3$ for each genotype). Venn diagram showing the number of shared and uniquely identified accessible peaks in *Npm1*$^{cA/+}$; *Swt* (green) and *Npm1*$^{cA/+}$; Shet (purple) HSPCs by ATAC sequencing. **D** HOMER analysis of the unique peaks in *Npm1*$^{cA/+}$; Shet HSPCs shows ETS family transcription factor sites are prevalent in the top five most enriched motifs by *p*-value. **E** IGV tracks of the *Fli1* gene showing enhanced accessibility (taller peaks) at the TSS in inv(16); *Shet* (in blue) vs. inv(16); *Swt* (in red) HSPCs. The scaling for all tracks displayed is identical. Additional peaks throughout the gene body and ~10 kb upstream of the TSS are observable in inv(16); *Shet* but not in inv(16); *Swt* cells. Regions of interest are boxed in green. mm10 was used for the genomic build. Tagpileup: top tracks for each genotype, Peaks called: bottom tracks for each genotype.

scored for every single cell (regulon activity score). Consistent with the upregulation of several Fli1 target genes (Fig. 3C), Fli1 was identified as a significantly enriched regulon (normalized enrichment score ≥ 3) in all cells from clusters 0, 1, 3, and 6 of our scRNA seq data, with 203 high-confidence Fli1-activated genes identified (Supplementary Table 4).

We hypothesized that there would be a quantitative difference in Fli1 regulon activity between the two genotypes, given the genotype-specific activation of select Fli1 targets observed in Fig. 3C. To address this hypothesis, we calculated the Z-score deviation from the average regulon activity score for the significant regulons that were also present as enriched motifs in our ATAC analysis from Fig. 2B. As shown in Fig. 5A, Fli1 showed a prominent Z-score increase in inv(16); *Shet* vs. inv(16); *Swt* cells (0.27 vs −0.22; $p = 2.2 \times 10^{-16}$), demonstrating that this regulon has increased activity in inv(16); *Shet* as compared to inv(16); *Swt* cells.

We next identified the *Fli1* level in the top quartile of inv(16); *Swt* cells from clusters 0, 1, 3, and 6 and then isolated inv(16); *Shet* cells with a similar high expression of *Fli1* (above the dashed line, Fig. 5B). This allowed us to isolate cells with comparable, high-level expression of *Fli1* under the two genetic conditions. We then plotted *Fli1* expression vs. regulon activity score for each cell to determine the relationship between the two (Fig. 5C). Applying a linear interaction model revealed a significant interaction between Fli1 regulon activity and genotype (Fig. 5C, $p = 2.89 \times 10^{-7}$). Post-hoc trend analysis showed that while Fli1 regulon activity was positively correlated with *Fli1* expression in both of the genotypes, the association was significantly more pronounced in the inv(16); *Shet* group compared to the inv(16); *Swt* group (inv(16); *Shet* slope = 1.9x that of inv(16); *Swt*). Collectively, our data indicate enhanced Fli1 target gene expression in *inv16; Shet* vs. *inv16; Swt* cells, even in cells where the expression level of *Fli1* itself is comparable between the two genotypes, suggesting that cohesin loss enhances the ability of Fli1 to drive gene expression on a per-cell basis. Our data support the hypothesis that re-enforced, deregulated Fli1 expression programs may contribute to the reduced latency observed in inv(16); *Shet* genotype by driving changes in gene expression in primitive hematopoietic progenitors.

Knockdown of Fli1 disrupts disease maintenance in inv(16);Shet leukemia

While our data demonstrate a potential role for Fli1 and its gene expression programs in accelerating inv(16);*Shet* leukemic development, we were curious if Fli1 also had a role during disease maintenance. Interestingly, the upregulation of Fli1 observed in HSPCs (Fig. 3B) was not maintained after leukemia development at either the mRNA or the protein level (Fig. 6A, B), suggesting that elevated Fli1 expression in response to *Smc3* haploinsufficiency occurs early, in the pre-leukemic state, and then wanes during leukemic progression. However, consistent expression of the Fli1 transcriptional program could still be required during the active disease stage. To determine if Fli1 is necessary for inv(16) leukemic maintenance, we lentivirally infected inv(16); *Shet* leukemic cells with an empty vector and two different shRNAs targeting Fli1 (shFli1). We achieved an approximate 70–80% knockdown at the mRNA level (data not shown) and 60–80% knockdown at the protein level (Supplementary Fig. 7A). We next transplanted 200,000 pLKO (empty vector/EV), shFli1 #1, or shFli1 #2 (all CD45.2) alongside 200,000 CD45.1 support cells into lethally irradiated CD45.1 recipients. Three mice for each condition were transplanted. All three mice receiving empty vector succumbed to leukemia 37 days post-transplant, while 5/6 mice receiving shFli1 #1 or shFli1 #2 did not present any evidence of leukemia 100 days post-transplant (Fig. 6C and Supplementary Fig. 7B). One shFli1 #1 recipient did have evidence of leukemia upon sacrifice 100 days post-transplant, including pale bones, an enlarged spleen, and excess blasts in the bone marrow (data not shown). As assessed by genotyping, the marrow of this animal was positive for inv(16) and *Smc3*$^{\Delta/+}$, indicating that the leukemia developed from the transplanted cells; however, a significant portion of the marrow was CD45.1+ (~60%, data not shown), indicating the leukemia was not as aggressive as in pLKO recipients. No CD45.2 cells were present in any of the five remaining shFli1 recipients (Supplementary Fig. 7C). We conclude that Fli1 expression is critical for inv(16); *Shet* leukemic maintenance.

Smc3 haploinsufficiency results in a more aggressive leukemic phenotype compared to inv(16) alone

We next sought to determine if overexpression of Fli1 would be sufficient to accelerate inv(16); *Swt* leukemogenesis. However, secondary transplants using lenti- or retrovirally infected HSPCs isolated from pIpC-treated inv(16) mice were not feasible due to poor engraftment, likely due to their reported poor contribution to the bone marrow in the presence of competitor cells, in this case, WT CD45.1 support cells [29]. We were therefore unable to definitively test if Fli1 accelerates inv(16)-driven leukemogenesis due to this technical limitation. Interestingly, similar to HSPCs, we also were unable to test the effect of Fli1 loss via shRNA-mediated depletion on inv(16);*Swt* disease maintenance due to poor engraftment of virally transduced inv(16);*Swt* leukemias. These data collectively suggest that *Smc3* heterozygosity is more detrimental to proper cell function in comparison to inv(16) alone.

DISCUSSION

In contrast to our initial hypothesis, we demonstrate reduced latency in inv(16); *Shet* vs. inv(16); *Swt* mice. While this manuscript was in revision, Conneely et al. published similar results, although statistical significance was not reached, likely due to a smaller number of mice used [44]. The reduced latency could be due to an accelerated rate of leukemogenesis or to a more aggressive disease maintenance stage. We were unfortunately unable to definitively show that Fli1 accelerates inv(16)-driven leukemogenesis due to poor engraftment of inv(16);*Swt* HSPCs. However, the enhanced expression of *Fli1* in primitive inv(16); *Shet* HSCs (Fig. 4D) combined with increased accessibility of Fli1 binding sites (Fig. 2B) and increased oncogenic, Fli1-mediated gene expression (Figs. 3C,

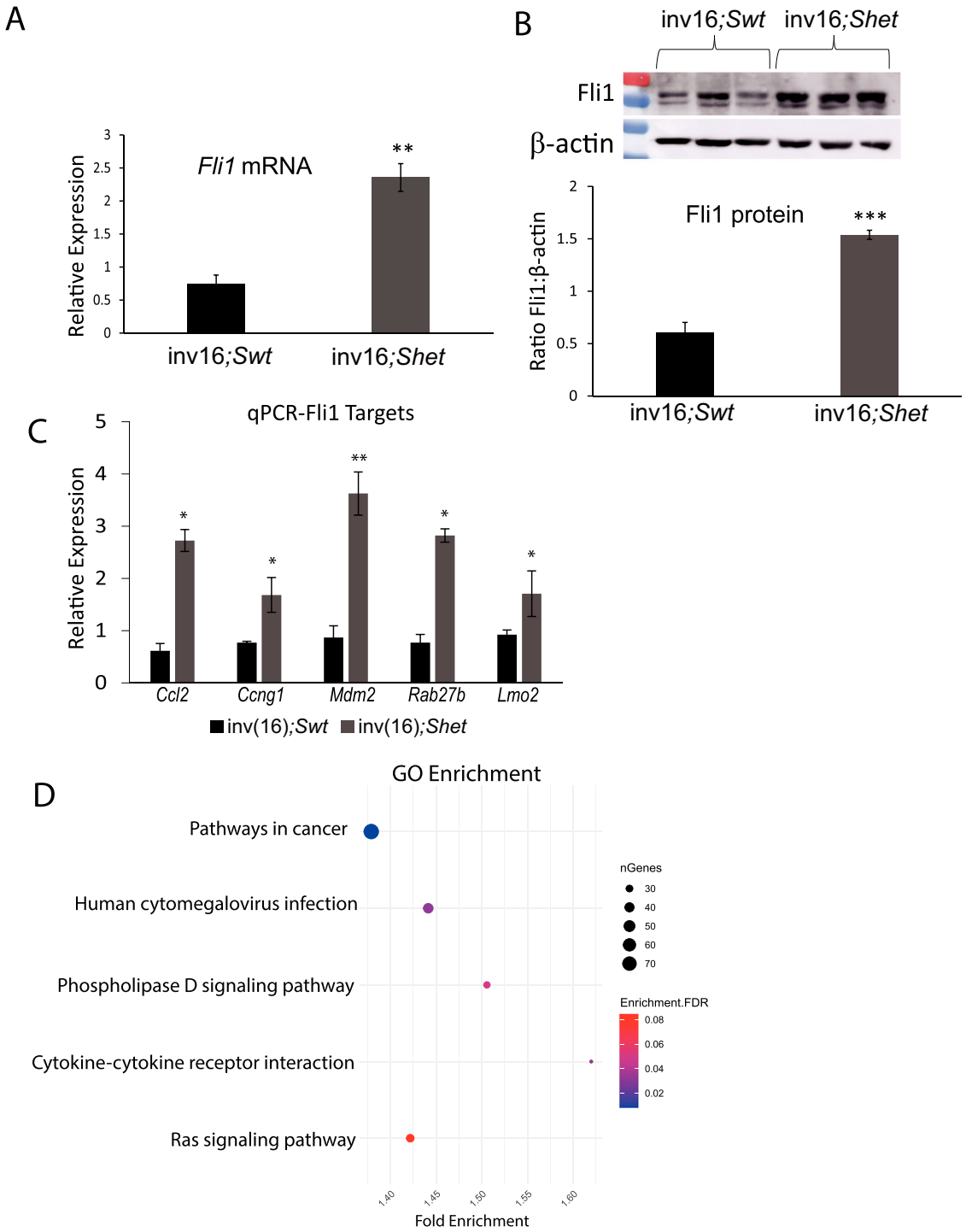

Fig. 3 ***Smc3* haploinsufficiency increases Fli1 expression and enhances Fli1 activity in pre-leukemic inv(16) HSPCs. A** qPCR was performed for *Fli1* mRNA on HSPCs isolated from inv(16); *Swt* and inv(16); *Shet* animals. The expression of *Fli1* was compared to β-*actin* as a control, and relative expression was plotted. **B** Western blot showing Fli1 protein expression for inv(16); *Swt* and inv(16); *Shet* HSPCs (top panel). *Fli1* expression was compared to β-actin as a control and quantified (lower panel). Due to the significant sequence homology between Fli1 and Erg, an antibody specific to Fli1 was used. **C** qPCR was performed for five known Fli1 transcription factor targets on inv(16); *Swt* and inv(16); *Shet* HSPCs. The expression of *Ccl1*, *Ccng1*, *Mdm2*, *Rab27b*, and *Lmo2* mRNA was compared to β-*actin* as a control and relative expression was plotted. **D** Fli1 binding sites were mapped to their nearest genes (+/− 50 kb) in the 33 133 unique peaks in inv(16); *Shet* and the 14 027 peaks shared between inv(16); *Swt* and inv(16); *Shet* from Fig. 2A. GO pathway analysis was performed using ShinyGO v0.80 for the inv(16); *Shet* genes, using the shared genes as background. The pathways were ranked from the largest to the smallest number of genes. Only those pathways with an FDR < 10% were retained. The top five pathways are shown. All assays in this figure were performed for three inv(16); *Swt* and three inv(16); *Shet* animals four weeks post-pIpC injection. *$p < 0.05$, **$p < 0.01$, ***$p < 0.001$, Student's *t* test. Data in A, B, C represent the mean +/− SEM.

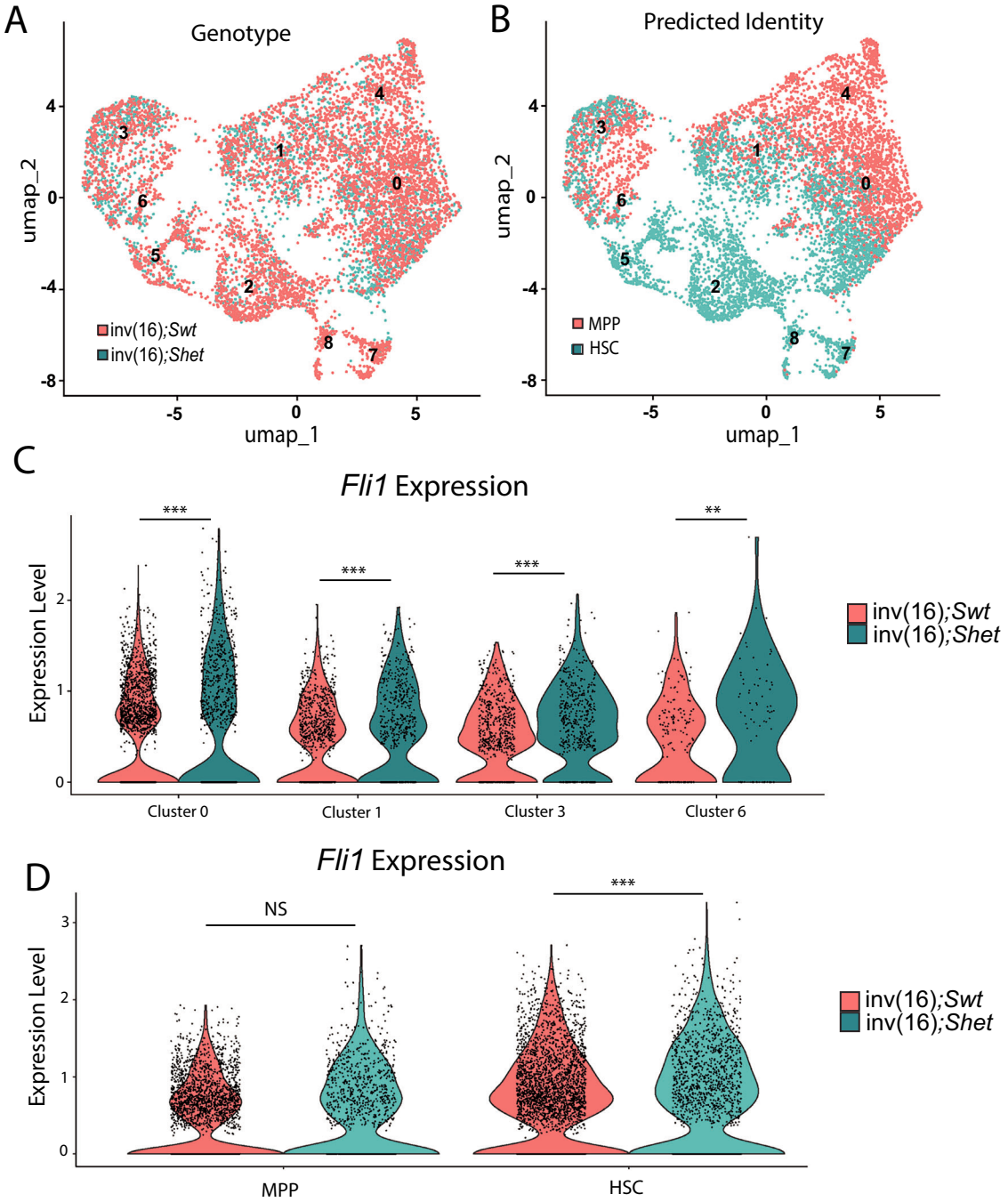

Fig. 4 Fli1 is overexpressed and drives an enhanced gene expression program in inv(16); *Shet* HSCs. A Seurat was used to group LSK-sorted cells from two inv(16); *Swt* and two inv(16); *Shet* into nine distinct clusters (0-8). Cells from inv(16); *Shet* mice are shown in blue, and those from inv(16); *Swt* mice are shown in salmon. In total, 2557 inv(16); *Shet* and 5 499 inv(16); *Swt* cells were used for analysis**. B** The SingleR tool was used to annotate the clusters using the Haemopedia mouse RNA sequencing reference transcriptomics dataset. **C** DESeq2 was used to test differential expression of *Fli1* in each cluster using a significance cutoff of adj. *p*-val <0.05. The expression levels of *Fli1* were plotted, and significantly increased expression was observed for inv(16); *Shet* cells (blue) vs. inv(16); *Swt* cells (red) in clusters 0, 1, 3, and 6. **D** DESeq2 was used to test differential expression of *Fli1* mRNA by cell type in clusters 0, 2, 3, and 6. Significantly increased *Fli1* expression was observed in inv(16); *Shet* (blue) vs. inv(16); *Swt* (red) HSCs. ***$p < 0.001$, **$p < 0.01$, Wilcoxon test.

D and 5A–C) in HSPCs suggest that Fli1 may contribute to a more rapid rate of disease initiation in the presence of inv(16), although additional experiments are required to rigorously distinguish the role of Fli1 in inv(16) leukemogenesis. Additionally, our data show a requirement for Fli1 in inv(16);*Shet* leukemias (Fig. 6C), indicating that *Smc3* haploinsufficiency likely reduces the latency of inv(16) AML due to effects on both the rate of leukemogenesis and the maintenance stage of disease. While we were unable to test the effect of Fli1 expression loss on inv(16); *Swt* disease maintenance due to poor long-term engraftment of virally transduced inv(16); *Swt* leukemias, our success in the inv(16); *Shet* genotype underscores the more aggressive nature of the *Shet* leukemias.

Given that Fli1 activation was associated with the expression of Ras pathway genes in inv(16); *Shet* cells (Figs. 2A, B; 3D), we hypothesize that this may contribute to an enhanced rate of leukemogenesis and/or increased robustness of the resulting

leukemia. RAS mutations are known to drive a more aggressive, more proliferative disease [45]. Interestingly, it has been proposed that mutated HSCs may be under chronic stress due to enhanced rates of proliferation or chronic inflammation, potentially resulting in epigenetic modifications that drive the acquisition of RAS mutations [45]. As the cohesin complex is known to regulate epigenetic changes and *Smc3* haploinsufficiency drives substantial changes in chromatin accessibility (Fig. 2A), it would be interesting to compare the epigenetic landscape of inv(16); *Shet* and inv(16); *RAS*-mutant cells, particularly with regard to sites of Fli1-mediated regulation. Examining changes in the epigenome may thus provide insight into why RAS mutations are more common in inv(16) vs. *t(8;21)* AML.

Of note, we and others [44] have not observed a big difference between leukemic inv(16); *Swt* and inv(16); *Shet* gene transcription via bulk RNAseq (data not shown). However, it is possible that scRNA sequencing may reveal changes in clonal heterogeneity and hierarchy between the two genotypes, and it is an important future experiment. While it is also possible that differences exist between mice and humans with regard to inv(16) AML leukemogenesis or maintenance, our results are consistent with

Table 1. Number of cells of each type analyzed by scRNAseq.

	Het	WT	Total
MPP	1075	2539	3614
STHSC	1482	2960	4442
Total	2557	5499	8056

The number of cells identified as MPPs or HSCs is noted for each genotype.

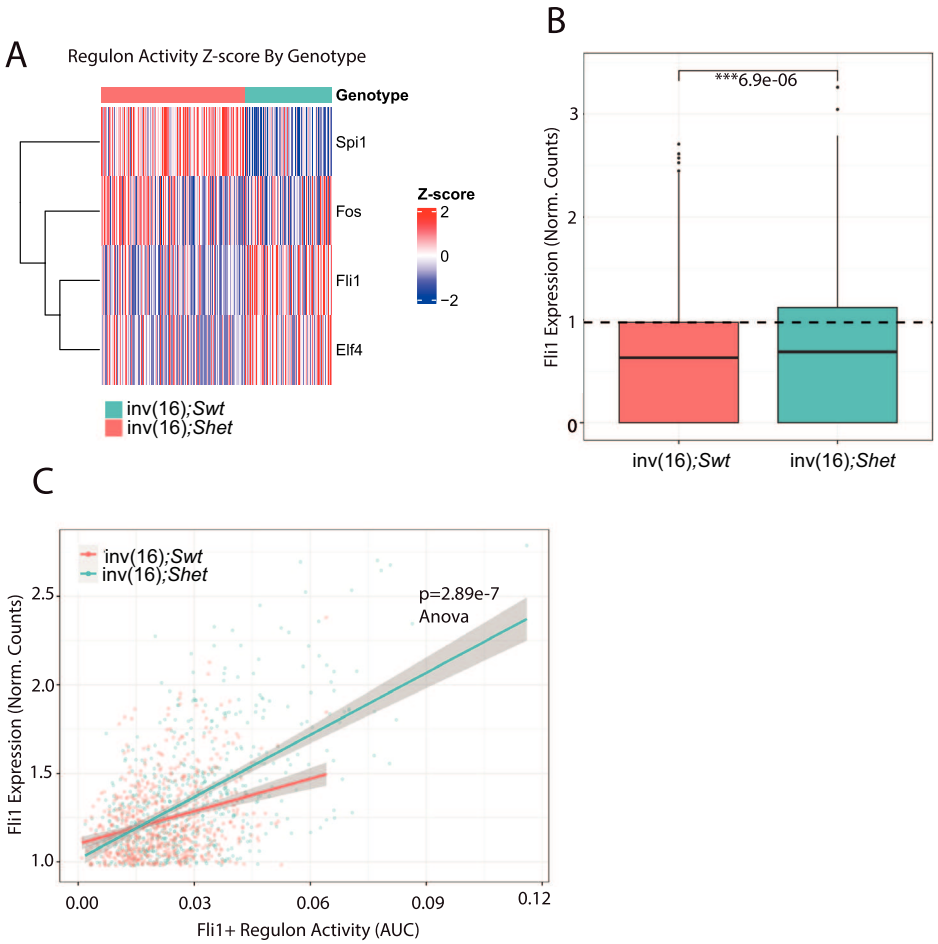

Fig. 5 The Fli1 regulatory network is a major contributor to gene expression in inv(16) HSCs. A PySCENIC was used to apply the mouse motif annotation database to our scRNA gene expression data. The area under the curve for each cell, representing the regulon activity score, was calculated with AUCell. Regulons that met a normalized enrichment score threshold ≥3, an AUC threshold of >0.05, and a rank threshold of 5000 were retained. The Z-score deviation from the AUC mean is shown in the heatmap for those motifs also identified by ATAC analysis in Fig. 2B. inv(16);*Swt* is shown in pink and inv(16);*Shet* in light blue. Average Z-score for inv(16);*Swt* = −0.22; Average Z-score for inv(16);*Shet* = 0.27. $p = 2.22 \times 10^{-16}$, Wilcoxon. **B** Box and whisker plot comparing log-normalized *Fli1* expression between inv(16); *Swt* (red) and inv(16); *Shet* (blue) in clusters 0, 1, 3, and 6. The central solid horizontal line represents the median, the box indicates the interquartile range (IQR), and the whiskers represent 1.5*IQR. Individual data points (dots) represent single-cell expression values. Statistical significance was determined by a two-tailed Wilcoxon rank-sum test ($p = 6.9 \times 10^{-6}$). $n = 5$ 650 total cells. The highest 25% of *Fli1*-expressing cells from inv(16); *Swt* and cells in inv(16); *Shet* with a similarly high expression level (above the dashed line) were taken for the analysis shown in (**C**). **C**. *Fli1* mRNA expression vs. regulon activity score from pySCENIC analysis was plotted for each genotype. Cells from inv(16); *Shet* mice are shown in blue, and those from inv(16); *Swt* mice are shown in red. 661 inv(16);*Swt* and 625 inv(16);*Shet* cells were used for the analysis. Linear regression models indicate a significant positive correlation in both genotypes; the regulatory slope is significantly steeper in inv(16); *Shet* cells (slope=11.71, $R^2 = 0.309$) compared to inv(16); *Swt* cells (slope=6.13, R2 = 0.091). Shaded areas represent 95% confidence intervals. Significance was tested with Anova ($p = 2.89 \times 10^{-7}$).

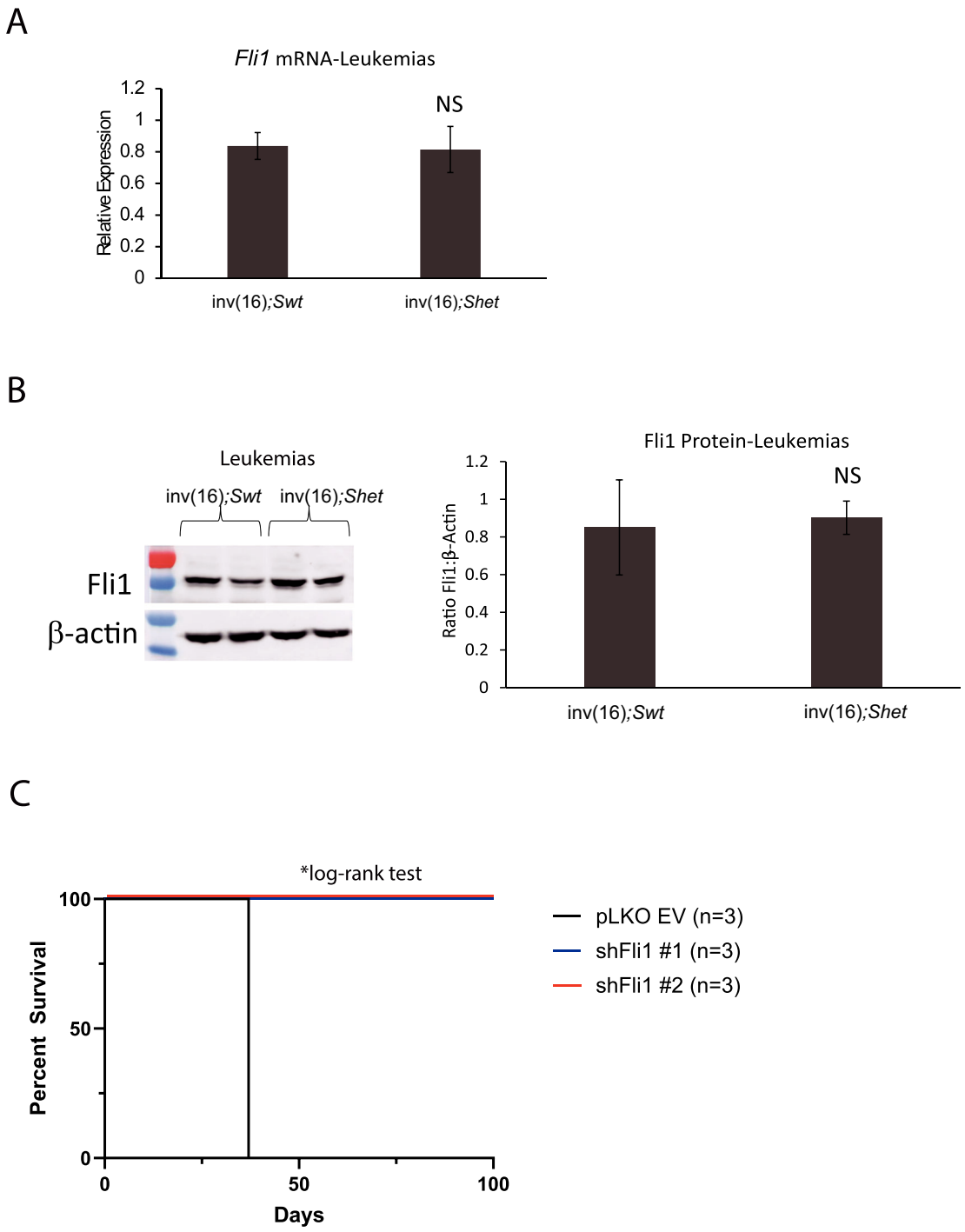

Fig. 6 Fli1 knockdown disrupts disease maintenance in inv(16); *Shet* leukemia. A qPCR was performed on cDNA from three inv(16); *Swt* and three inv(16); *Shet* leukemias for *Fli1* mRNA using β-*actin* as a control. The relative expression for each genotype was plotted. **B** Western blot showing the expression level of Fli1 protein vs. β-actin in two inv(16); *Swt* and two inv(16); *Shet* leukemias (left panel). The expression of Fli1 vs. β-actin was quantified and plotted (right panel). **C** Survival curve showing mice receiving pLKO (empty vector, EV, black), shFli1#1 (blue), and shFli1 #2 (red, overlaps with blue). $n = 3$ for each condition, $*p < 0.01$, log-rank test. Data in A and B represent the mean +/− SEM. NS: non-significant, Student's *t* test.

previously published effects of Fli1 in a variety of AML and MDS models [46–50].

How might *Smc3*$^{\Delta/+}$ and inv(16) cooperate to enhance Fli1 activity? We have previously shown that cohesin recruits the histone methylase complex, PRC2, to repress *Hoxa7/9* [25]. Under cohesin haploinsufficiency, the repressive mark H3K27me3 is lost at the *Hoxa7/9* promoters, resulting in increased expression, driving self-renewal [25]. Additional studies have shown that loss of the cohesin subunit *STAG2* results in a decrease in the H3K27me3 mark at multiple sites [51]. As the *FLI1* promoter is a target of PRC2 in breast cancer [52], we hypothesize that *Smc3*$^{\Delta/+}$ may result in a loss of PRC2-mediated methylation at the *Fli1* promoter, driving enhanced expression. Additionally, the CBFB-SMMHC fusion has been shown to interact with the transcriptional coactivator p300 and other hematopoietic transcription factors, including TAL1, ELF1, ERG, and PU.1 [32], which may further drive

FLI1 and FLI1-mediated gene expression changes. While the comprehensive effects of Fli1 regulon activation in AML are unknown, Fli1 regulates multiple factors involved in myeloid differentiation, self-renewal, and proliferation [46–48, 53]. Collectively, the literature and our data suggest that cohesin haploinsufficiency results in increased *Fli1* expression and Fli1 site accessibility, allowing the CBFβ::SMMHC fusion and Fli1 to cooperatively deregulate gene expression to drive a reduction in disease latency. The negative impact of *FLI1* upregulation is evidenced by previous studies linking deregulated *FLI1* expression with reduced overall survival and duration of remission in AML [48, 49]. Therefore, we speculate that patients with enhanced FLI1 activity, and not simply elevated *FLI1* expression, may have an overall worse prognosis.

Interestingly, about half of all patients with an *NPM1*^{cA} mutation also harbor a cohesin mutation [4, 21, 22], and patients with mutated *NPM1* or *FLT3-ITD* have been documented to have higher Fli1 protein expression and lower overall survival [49]. Similar to inv(16); *Shet* cells, we observed an enrichment of Fli1-binding motifs in the uniquely accessible chromatin regions in *Npm1*$^{cA/+}$; *Smc3*$^{\Delta/+}$ HSPCs (Fig. 2D), indicating that Fli1 may be a specific target for cohesin-mutated AMLs. Interestingly, others have identified Fli1 as a putative target in erythroleukemia, where it has been shown to regulate proliferation, inflammation, apoptosis, differentiation, and angiogenesis [53–55]. Several molecules with varying levels of specificity have been shown to inhibit Fli1, with the EWS-FLI1 inhibitor trabectedin (ET-743) receiving FDA approval for the treatment of ovarian cancer and soft-tissue sarcomas, and TK216 completing phase I/II trials for Ewing sarcoma [56, 57]. However, significant difficulties persist in identifying a Fli1-specific inhibitor that is clinically efficacious and lacks significant off-target effects. Further, it is unknown if EWS-FLI1 inhibitors will also target wild-type Fli1, which appears to be critical in inv(16) leukemia based upon the data presented here. Additional studies with co-mutational models may aid in achieving mechanistic insights for newer classes of Fli1 inhibitors and will be necessary to explore how broadly related Fli1 expression programs are to cohesin loss.

Given the decreased latency we observed upon combining *Smc3* haploinsufficiency and inv(16), it is surprising that cohesin mutations are not commonly found alongside inv(16) mutations in AML. It is possible that cohesin mutations co-occur in concert with inv(16) at a higher rate than has been reported. Targeted amplicon sequencing with higher coverage revealed additional mutations in 96% of patients in one CBF AML study [16]. In this study, a total of six cohesin mutations were found by targeted sequencing in inv(16) AML samples, which were not observed by whole exome sequencing [16]. We combined the six cohesin-mutated samples into one group to analyze the effect of cohesin mutation on overall survival or recurrence-free survival vs. cohesin-WT inv(16) AML, but found no difference (Supplementary Fig. 8A, B), likely due to the low number of cohesin-mutated samples. Thus, targeted sequencing of more patient samples may uncover additional cohesin mutations in inv(16) and add more power to this analysis. Our mechanistic data do, however, provide an alternative hypothesis as to why inv(16) and cohesin mutations are rarely observed together. We have shown that the addition of *Smc3* haploinsufficiency results in a dramatic increase in chromatin accessibility, with an enrichment of Fli1 binding sites linked to RAS signaling genes (Fig. 2A, B; 3D). The most common co-occurring mutations with inv(16) are activating mutations in *N-RAS* or *K-RAS* [15–19], suggesting that inv(16); *Shet* may mimic some effects of RAS mutations, although not at the level of RAS itself (Supplementary Fig. 5C). In support of this, most prostate cancers do not have *RAS* mutations, but ~50% express aberrant fusions between *TMPSS2* and ETS family members [58, 59]. While fusion with *FLI1* is rare [58], fusion-mediated overexpression of ETS family members can drive transformation and activate a cell migration gene expression program normally driven by RAS, even in the absence of RAS signaling [59]. Thus, ETS family overexpression in prostate cancer can mimic RAS pathway activation [59]. We speculate that *Smc3* haploinsufficiency may partially mimic RAS-activating mutations often seen in inv(16) leukemias through overactivation of Fli1 and its targets. As active *RAS* mutations are strong leukemic drivers, their early acquisition in inv(16) AML likely makes selection of cohesin mutations redundant. Further studies on how cohesin, the core binding factor complex, and Fli1 cooperate to regulate inv(16) leukemia will likely uncover additional mechanisms common to AML development and progression.

DATA AVAILABILITY

All sequencing data have been deposited in GEO Omnibus under the accession numbers: ATAC-seq GSE286322, Reviewer Access Token: uhyhwkccrtwrpsj; scRNA-seq GSE286946, Reviewer Access Token: enihwaeqdrufjuj; ATAC-seq GSE286947, Reviewer Access Token: ofmnecucvbezrkp.

REFERENCES

1. Chen P, Liu X, Zhao Y, Hu Y, Guo J, Wang H. Global, national, and regional burden of acute myeloid leukemia among 60–89 years-old individuals: insights from a study covering the period 1990 to 2019. Front Public Health. 2024;11:1329529.
2. Patel JP, Gönen M, Figueroa ME, Fernandez H, Sun Z, Racevskis J, et al. Prognostic relevance of integrated genetic profiling in acute myeloid leukemia. N Engl J Med. 2012;366:1079–89.
3. Papaemmanuil E, Gerstung M, Bullinger L, Gaidzik VI, Paschka P, Roberts ND, et al. Genomic classification and prognosis in acute myeloid leukemia. N Engl J Med. 2016;374:2209–21.
4. Network TCGAR. Genomic and epigenomic landscapes of adult de novo acute myeloid leukemia. N Engl J Med. 2013;368:2059–74.
5. Tyner JW, Tognon CE, Bottomly D, Wilmot B, Kurtz SE, Savage SL, et al. Functional genomic landscape of acute myeloid leukaemia. Nature. 2018;562:526–31.
6. Sargas C, Ayala R, Larrayoz MJ, Chillon MC, Carrillo-Cruz E, Bilbao-Sieyro C, et al. Molecular landscape and validation of new genomic classification in 2668 adult AML patients: real- life data from the PETHEMA registry. Cancers. 2023;15:438.
7. Borthakur G, Kantarjian H. Core binding factor acute myelogenous leukemia-2021 treatment algorithm. Blood Cancer J. 2021;11:114.
8. Quan X, Deng J. Core binding factor acute myeloid leukemia: advances in the heterogeneity of KIT, FLT3, and RAS mutations (Review). Mol Clin Oncol. 2020;13:95–100.
9. Darwish C, Farina K, Tremblay D. The core concepts of core binding factor acute myeloid leukemia: current considerations for prognosis and treatment. Blood Rev. 2023;62:101117.
10. Beghini A. Core binding factor leukemia: chromatin remodeling moves towards oncogenic transcription. Cancers. 2019;11:1973.
11. Surapally S, Tenen DG, Pulikkan JA. Emerging therapies for inv(16) AML. Blood. 2021;137:2579–84.
12. Xue L, Pulikkan JA, Valk PJM, Castilla LH. NrasG12D oncoprotein inhibits apoptosis of preleukemic cells expressing Cbfβ-SMMHC via activation of MEK/ERK axis. Blood. 2014;124:426–36.
13. Castilla LH, Wijmenga C, Wang Q, Stacy T, Speck NA, Eckhaus M, et al. Failure of embryonic hematopoiesis and lethal hemorrhages in mouse embryos heterozygousfor a knocked-in leukemia gene CBFB–MYH11. Cell. 1996;87:687–96.
14. Day RB, Hickman JA, Xu Z, Katerndahl CDS, Ferraro F, Ramakrishnan SM, et al. Proteogenomic analysis reveals cytoplasmic sequestration of RUNX1 by the acute myeloid leukemia–initiating CBFB::MYH11 oncofusion protein. J Clin Investig. 2024;134:e176311.
15. Faber ZJ, Chen X, Gedman AL, Boggs K, Cheng J, Ma J, et al. The genomic landscape of core-binding factor acute myeloid leukemias. Nat Genet. 2016;48:1551–6.
16. Opatz S, Bamopoulos SA, Metzeler KH, Herold T, Ksienzyk B, Braundl K, et al. The clinical mutatome of core binding factor leukemia. Leukemia. 2020;34:1553–62.
17. Duployez N, Marceau-Renaut A, Boissel N, Petit A, Bucci M, Geffroy S, et al. Comprehensive mutational profiling of core binding factor acute myeloid leukemia. Blood. 2016;127:2451–9.
18. Jahn N, Terzer T, Strang E, Dolnik A, Cocciardi S, Panina E, et al. Genomic heterogeneity in core-binding factor acute myeloid leukemia and its clinical implications. Blood Adv. 2020;4:6342–52.

19. Qin W, Chen X, Shen HJ, Wang Z, Cai X, Jiang N, et al. Comprehensive mutation profile in acute myeloid leukemia patients with RUNX1-RUNX1T1 or CBFB-MYH11 fusions. Turk J Haematol. 2022;39:84–93.
20. Kong X, Ball AR Jr., Pham HX, Zeng W, Chen HY, Schmiesing JA, et al. Distinct functions of human cohesin-SA1 and cohesin-SA2 in double-strand break repair. Mol Cell Biol. 2014;34:685–98.
21. Heimbruch KE, Meyer AE, Agrawal P, Viny AD, Rao S. A cohesive look at leukemogenesis: the cohesin complex and other driving mutations in AML. Neoplasia. 2021;23:337–47.
22. Thol F, Bollin R, Gehlhaar M, Walter C, Dugas M, Suchanek KJ, et al. Mutations in the cohesin complex in acute myeloid leukemia: clinical and prognostic implications. Blood. 2014;123:914–20.
23. Thota S, Viny AD, Makishima H, Spitzer B, Radivoyevitch T, Przychodzen B, et al. Genetic alterations of the cohesin complex genes in myeloid malignancies. Blood. 2014;124:1790–8.
24. Kon A, Shih LY, Minamino M, Sanada M, Shiraishi Y, Nagata Y, et al. Recurrent mutations in multiple components of the cohesin complex in myeloid neoplasms. Nat Genet. 2013;45:1232–7.
25. Fisher JB, Peterson J, Reimer M, Stelloh C, Pulakanti K, Gerbec ZJ, et al. The cohesin subunit Rad21 is a negative regulator of hematopoietic self-renewal through epigenetic repression of Hoxa7 and Hoxa9. Leukemia. 2017;31:712–9.
26. Viny AD, Ott CJ, Spitzer B, Rivas M, Meydan C, Papalexi E, et al. Dose-dependent role of the cohesin complex in normal and malignant hematopoiesis. J Exp Med. 2015;212:1819–32.
27. Mullenders J, Aranda-Orgilles B, Lhoumaud P, Keller M, Pae J, Wang K, et al. Cohesin loss alters adult hematopoietic stem cell homeostasis, leading to myeloproliferative neoplasms. J Exp Med. 2015;212:1833–50.
28. Mazumdar C, Shen Y, Xavy S, Zhao F, Reinisch A, Li R, et al. Leukemia-associated cohesin mutants dominantly enforce stem cell programs and impair human hematopoietic progenitor differentiation. Cell Stem Cell. 2015;17:675–88.
29. Kuo Y-H, Landrette SF, Heilman SA, Perrat PN, Garrett L, Liu PP, et al. Cbfβ-SMMHC induces distinct abnormal myeloid progenitors able to develop acute myeloid leukemia. Cancer Cell. 2006;9:57–68.
30. Meyer AE, Stelloh C, Pulakanti K, Burns R, Fisher JB, Heimbruch KE, et al. Combinatorial genetics reveals the Dock1-Rac2 axis as a potential target for the treatment of NPM1; cohesin-mutated AML. Leukemia. 2022;36:2032–41.
31. Viny AD, Bowman RL, Liu Y, Lavallee VP, Eisman SE, Xiao W, et al. Cohesin members Stag1 and Stag2 display distinct roles in chromatin accessibility and topological control of HSC self-renewal and differentiation. Cell Stem Cell. 2019;25:682–96 e8.
32. Mandoli A, Singh AA, Jansen PW, Wierenga AT, Riahi H, Franci G, et al. CBFB-MYH11/RUNX1 together with a compendium of hematopoietic regulators, chromatin modifiers and basal transcription factors occupies self-renewal genes in inv(16) acute myeloid leukemia. Leukemia. 2014;28:770–8.
33. Laudet V, Hanni C, Stehelin D, Duterque-Coquillaud M. Molecular phylogeny of the ETS gene family. Oncogene. 1999;18:1351–9.
34. Kamikubo Y, Zhao L, Wunderlich M, Corpora T, Hyde RK, Paul TA, et al. Accelerated leukemogenesis by truncated CBFβ-SMMHC defective in high-affinity binding with RUNX1. Cancer Cell. 2010;17:455–68.
35. Czeh M, Rosenbauer F. Uncovering a new cellular origin for acute myeloid leukemia with lineage plasticity. Mol Cell Oncol. 2017;4:e1268241.
36. Chen Y, Li J, Xu L, Găman M-A, Zou Z. The genesis and evolution of acute myeloid leukemia stem cells in the microenvironment: from biology to therapeutic targeting. Cell Death Discov. 2022;8:397.
37. George J, Uyar A, Young K, Kuffler L, Waldron-Francis K, Marquez E, et al. Leukaemia cell of origin identified by chromatin landscape of bulk tumour cells. Nat Commun. 2016;7:12166.
38. Mayle A, Luo M, Jeong M, Goodell MA. Flow cytometry analysis of murine hematopoietic stem cells. Cytom Part A. 2013;83A:27–37.
39. Challen GA, Boles N, Lin KYK, Goodell MA. Mouse hematopoietic stem cell identification and analysis. Cytom Part A. 2009;75A:14–24.
40. Shao L, Wang Y, Chang J, Luo Y, Meng A, Zhou D. Hematopoietic stem cell senescence and cancer therapy-induced long-term bone marrow injury. Transl Cancer Res. 2013;2:397–411.
41. Choi J, Baldwin TM, Wong M, Bolden JE, Fairfax KA, Lucas EC, et al. Haemopedia RNA-seq: a database of gene expression during haematopoiesis in mice and humans. Nucleic Acids Res. 2019;47:D780–D785.
42. Pulikkan JA, Castilla LH. Preleukemia and leukemia-initiating cell activity in inv(16) acute myeloid leukemia. Front Oncol. 2018;8:129.
43. Van de Sande B, Flerin C, Davie K, De Waegeneer M, Hulselmans G, Aibar S, et al. A scalable SCENIC workflow for single-cell gene regulatory network analysis. Nat Protoc. 2020;15:2247–76.
44. Conneely SE, Quezada A, Kurtz KJ, Zhang N, Fuente J, Mercer N, et al. Cohesin haploinsufficiency is tolerated in Cbfb: MYH11-driven murine acute myeloid leukemia. Exp Hematol. 2026;153:105287.
45. Alawieh D, Cysique-Foinlan L, Willekens C, Renneville A. RAS mutations in myeloid malignancies: revisiting old questions with novel insights and therapeutic perspectives. Blood Cancer J. 2024;14:72.
46. Thoms JAI, Truong P, Subramanian S, Knezevic K, Harvey G, Huang Y, et al. Disruption of a GATA2-TAL1-ERG regulatory circuit promotes erythroid transition in healthy and leukemic stem cells. Blood. 2021;138:1441–55.
47. Nagel S, Pommerenke C, Meyer C, Macleod RAF. NKL homeobox genes NKX2-3 and NKX2-4 deregulate megakaryocytic-erythroid cell differentiation in AML. Int J Mol Sci. 2021;22:11434.
48. Xiang P, Yang X, Escano L, Dhillon I, Schneider E, Clemans-Gibbon J, et al. Elucidating the importance and regulation of key enhancers for human MEIS1 expression. Leukemia. 2022;36:1980–9.
49. Kornblau SM, Qiu YH, Zhang N, Singh N, Faderl S, Ferrajoli A, et al. Abnormal expression of FLI1 protein is an adverse prognostic factor in acute myeloid leukemia. Blood. 2011;118:5604–12.
50. Ochi Y, Kon A, Sakata T, Nakagawa MM, Nakazawa N, Kakuta M, et al. Combined cohesin–RUNX1 deficiency synergistically perturbs chromatin looping and causes myelodysplastic syndromes. Cancer Discov. 2020;10:836–53.
51. Adane B, Alexe G, Seong BKA, Lu D, Hwang EE, Hnisz D, et al. STAG2 loss rewires oncogenic and developmental programs to promote metastasis in Ewing sarcoma. Cancer Cell. 2021;39:827–44.e10.
52. Cai Y, Lin J-R, Zhang Q, O'Brien K, Montagna C, Zhang ZD. Epigenetic alterations to Polycomb targets precede malignant transition in a mouse model of breast cancer. Sci Rep. 2018;8:5535.
53. Ben-David Y, Gajendran B, Sample KM, Zacksenhaus E. Current insights into the role of Fli-1 in hematopoiesis and malignant transformation. Cell Mol Life Sci. 2022;79:163.
54. Liu T, Xia L, Yao Y, Yan C, Fan Y, Gajendran B, et al. Identification of diterpenoid compounds that interfere with Fli-1 DNA binding to suppress leukemogenesis. Cell Death Dis. 2019;10:117.
55. Li YJ, Zhao X, Vecchiarelli-Federico LM, Li Y, Datti A, Cheng Y, et al. Drug-mediated inhibition of Fli-1 for the treatment of leukemia. Blood Cancer J. 2012;2:e54.
56. Grohar PJ, Griffin LB, Yeung C, Chen QR, Pommier Y, Khanna C, et al. Ecteinascidin 743 interferes with the activity of EWS-FLI1 in Ewing sarcoma cells. Neoplasia. 2011;13:145–53.
57. Meyers PA, Federman N, Daw N, Anderson PM, Davis LE, Kim A, et al. Open-label, multicenter, phase I/II, first-in-human trial of TK216: a first-generation EWS::FLI1 fusion protein antagonist in Ewing sarcoma. J Clin Oncol. 2024;42:3725–34.
58. Paulo P, Barros-Silva JD, Ribeiro FR, Ramalho-Carvalho J, Jerónimo C, Henrique R, et al. FLI1 is a novel ETS transcription factor involved in gene fusions in prostate cancer. Genes, Chromosomes, Cancer. 2012;51:240–9.
59. Selvaraj N, Budka JA, Ferris MW, Jerde TJ, Hollenhorst PC. Prostate cancer ETS rearrangements switch a cell migration gene expression program from RAS/ERK to PI3K/AKT regulation. Mol Cancer. 2014;13:61.

ACKNOWLEDGEMENTS

The authors would like to acknowledge the Versiti Research Institute Shared Resources Core Facility (RRID # SCR_025503) supported by the Versiti Blood Research Institute Foundation, for their services, instrumentation and specialist support. In particular, we would like to thank Benedetta Bonacci, Savannah Neu, and Rebekah Doerfler for aid with flow cytometry experiments, as well as Barbara Flemming and Nicole Leon for histology work. This work was partially funded by: NCI R01 CA204231, NHLBI PO1 HL149620, and NIDDK R01 DK134064 to S. Rao and NCI F30 CA236322 to K Heimbruch.

AUTHOR CONTRIBUTIONS

Alison E Meyer designed research studies, conducted experiments, acquired and analyzed data, and wrote the manuscript. Katelyn E Heimbruch designed research studies, conducted experiments, and acquired and analyzed data. Kirthi Pulakanti analyzed data. Nataly Cruz-Rodriguez conducted experiments. Cary Stelloh and Josiah Murray conducted experiments and acquired data. Sebastian Vosberg, Lisa Latzko, and Philipp A Greif analyzed data and provided comments and edits to the manuscript. Lucio Castilla provided a mouse model for the experiments and provided comments and edits to the manuscript. John A Pulikkan, Dandan Wang, and Subramaniam Malarkannan provided critical advice on data analysis and experiment design and contributed comments and edits to the manuscript. Sridhar Rao designed research studies and aided in writing the manuscript.

FUNDING

This work was partially funded by: NCI R01 CA204231, NHLBI PO1 HL149620, and NIDDK R01 DK134064 to S. Rao and NCI F30 CA236322 to K. Heimbruch.

COMPETING INTERESTS

The authors declare no competing interests.

ADDITIONAL INFORMATION

Supplementary information The online version contains supplementary material available at https://doi.org/10.1038/s41375-026-03070-6.

Correspondence and requests for materials should be addressed to Sridhar Rao.

Reprints and permission information is available at http://www.nature.com/reprints

Publisher's note Springer Nature remains neutral with regard to jurisdictional claims in published maps and institutional affiliations.

Open Access This article is licensed under a Creative Commons Attribution-NonCommercial-NoDerivatives 4.0 International License, which permits any non-commercial use, sharing, distribution and reproduction in any medium or format, as long as you give appropriate credit to the original author(s) and the source, provide a link to the Creative Commons licence, and indicate if you modified the licensed material. You do not have permission under this licence to share adapted material derived from this article or parts of it. The images or other third party material in this article are included in the article's Creative Commons licence, unless indicated otherwise in a credit line to the material. If material is not included in the article's Creative Commons licence and your intended use is not permitted by statutory regulation or exceeds the permitted use, you will need to obtain permission directly from the copyright holder. To view a copy of this licence, visit http://creativecommons.org/licenses/by-nc-nd/4.0/.

© The Author(s) 2026